The Network of Receptors Characterize B Cell Receptor Micro- and Macroclustering in a Monte Carlo Model

ARTICLE *in* THE JOURNAL OF PHYSICAL CHEMISTRY B · DECEMBER 2009

Impact Factor: 3.3 · DOI: 10.1021/jp9079074 · Source: PubMed

The Network of Receptors Characterize B Cell Receptor Micro- and Macroclustering in a Monte Carlo Model

A. Srinivas Reddy,[†] Sandeep Chilukuri,[†,‡] and Subhadip Raychaudhuri*[,†,§,∥,⊥]

Department of Biomedical Engineering, Biophysics Graduate Group, Graduate Group in Immunology, and Graduate Group in Applied Mathematics, University of California—Davis, Davis, California, and Department of Biotechnology, Indian Institute of Technology Madras, Chennai, India

Received: August 15, 2009; Revised Manuscript Received: November 4, 2009

During the recognition of soluble antigens, B cell receptors (BCR) are known to form signaling clusters that can crucially modulate intracellular activation pathways and B cell response. Little is known about the precise nature of receptor cluster and its formation mechanism for the case of soluble antigens. Initial experiments have shown that B cell receptors first microcluster upon ligation with soluble antigens, and then coarsen into a macroscopic *cap* structure at one pole of a B cell. Such a mutual receptor—receptor attraction can arise locally due to cross-linking by soluble antigens among other possibilities. We develop an energy based Monte Carlo model to investigate the mechanism of B-cell receptor clustering upon ligation with soluble antigens. Our results show that mutual attraction between nearest neighbor receptor pairs can lead to microclustering of B cell receptors, but it is not sufficient for receptor macroclustering. A simple model of biased diffusion where BCR molecules experience a biased directed motion toward the largest cluster is then applied, which results in a single macrocluster of receptor molecules. The various types of receptor clusters are analyzed using the developed network-based metrics such as the average distance between any pairs of receptors.

Introduction

Clustering of membrane-bound receptor molecules can be taken as a signaling motif that helps recognize external stimuli and crucially modulates cellular response through the activation of intracellular signaling pathways.[1−3] In immune cells, such receptor clustering can be crucial to antigen recognition and immune activation.[4−6] In B and T lymphocytes, for example, it has been shown that immune receptors cluster in the form of an *immunological synapse* pattern during the recognition of membrane-bound antigens.[7−10] A lot of recent experimental and theoretical efforts have been devoted to elucidate the mechanisms of such pattern formation for the case of membrane-bound antigens.[8−16] In contrast, little is known about the mechanism of B cell receptor (BCR) clustering during the recognition of soluble antigens. It is known that B cell receptors cluster in the form of a *cap* at one pole of a cell during the recognition of soluble antigens.[17] It has also been shown that B cell receptors first microcluster upon cross-linking by soluble antigens and then at a later stage those microclusters coalesce into a large macroscopic cluster in the form of a cap.[11] Membrane domains (or rafts) that are enriched in sphingolipids and cholesterol have been implicated in such receptor "capping".[18]

Lack of a large number of experimental studies on B cell receptor clustering, during the recognition of soluble antigens, makes its mechanistic exploration challenging. In this Article, we study a model of BCR clustering that is mediated by mutual attraction between BCR molecules. Such mutual receptor—receptor attraction can arise due to antigen cross-linking, increased raft association of BCRs upon antigen binding, or some other biophysical mechanisms.[11,19−21] We use an energy-function-based Monte Carlo algorithm to study receptor clustering due to mutual attraction between receptors. We vary the strength of the attractive interaction as well as the density of molecules in our simulations. Nearest neighbor attraction among receptors placed on a square lattice is shown to be enough for receptor microclustering. A very high density of receptors also leads to receptor macroclustering, but such high receptor density may not be physiological. We simulate a mechanism of directed diffusion where BCR molecules move toward the largest microcluster with a diffusion bias. Such biased diffusion readily macrocluster B cell receptors, as seen in cap formation.

On the basis of the spatial organization of receptor networks on the cell surface, we develop some quantitative criteria to characterize different types of B cell receptor clustering. We first consider the average pairwise distance among all of the receptors, which shows some simple functional relationship with the number of receptors for the extreme cases of receptor random distribution and receptor macroclustering. An alternative metric, which is based on the total number of nearest neighbor receptor pairs, also shows simple scaling with the total number of receptors. Our Monte Carlo simulations verify the receptor-network-based quantitative relations, which are derived using simple geometrical arguments.

Methods

We carry out energy-based Monte Carlo simulations to model mutual receptor—receptor attraction on the B cell surface. The total energy (Hamiltonian) of the system is given by

* To whom correspondence should be addressed. E-mail: raychaudhuri@ucdavis.edu.
† Department of Biomedical Engineering, University of California—Davis.
‡ Indian Institute of Technology Madras.
§ Biophysics Graduate Group, University of California—Davis.
∥ Graduate Group in Immunology, University of California—Davis.
⊥ Graduate Group in Applied Mathematics, University of California—Davis.

10.1021/jp9079074
Published on Web 12/15/2009

$$H = -K\sum_{i,j} S_i S_j$$

S can take two values: 0 (no receptor) and 1 (receptor occupied). i and j are the nearest neighbor sites for which mutual receptor attractions are considered. The constant parameter K in the energy function represents the strength of an attractive interaction that is varied in our simulations. A total of four/eight neighboring sites are included in evaluating the energy.[3]

Initially, the cell receptor molecules are placed randomly on a cell surface. We pick up a molecule randomly on the cell surface and attempt a diffusion move to any of the four neighboring sites. In each Monte Carlo move, neighboring sites of a molecule are chosen with equal probability and a diffusion move can be made only when the chosen site is not already occupied by another molecule. Finally, the diffusion move to a new neighboring site is accepted with an energy-based criterion (as depicted in Figure 1). One Monte Carlo time step consists of N repeated single molecule moves, where N is the total number of molecules.

When a receptor is moved to a new site with a bigger number of neighboring receptors, the total energy is lowered and such a move is preferred. When we used the Metropolis algorithm with probability $(P) = \min(1, e^{-\beta\Delta E})$, it showed little or no microclustering for a long time. This happens as most diffusion moves in this Metropolis scheme do not result in an increase in the number of neighbor receptors, thus making the algorithm slow to reach a microclustered state. To remedy this problem, we devised a novel energy-based scheme that can make the system move faster to equilibrium configurations. In this proposed algorithm, we sampled the energy landscape with Monte Carlo moves that gives a higher weight to moves that decreases the energy more. Thus, diffusion moves that result in a bigger change in energy are preferred. In this scheme, molecules are moved to a new position with a probability max of $(0, e^{(1/2)\beta\Delta E}/e^{(1/2)\beta\Delta E_{max}})$. This proposed Monte Carlo algorithm satisfies the dual criteria of ergodicity and detailed balance.[22] This Monte Carlo scheme also satisfies the detailed balance condition

$$\frac{P_{1\to 2}}{P_{2\to 1}} = \frac{e^{(1/2)\beta\Delta E_{12}}}{e^{(1/2)\beta\Delta E_{21}}} = e^{-\beta(E_2 - E_1)}$$

Hence, the move that leads to the maximum lowering in energy is performed with a probability of 1; thus, it is the most preferred move in this algorithm. Other moves are carried out with a probability smaller than 1 and depend on the change in energy of the system. Diffusion moves that will result in zero energy change will also be carried out with a probability lower than 1 (scaled by E_{max}).

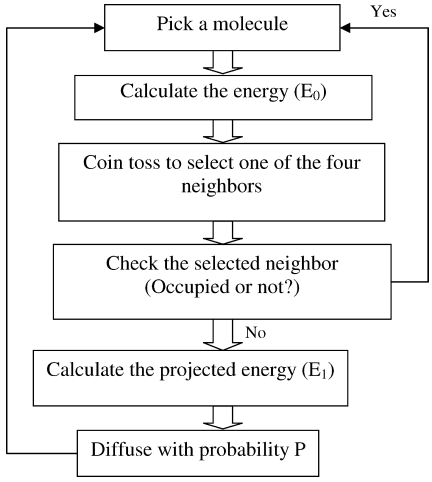

Figure 1. Flowchart depicting the Monte Carlo algorithm used.

Results

Mutual Receptor−Receptor Attraction Leads to Receptor Microclustering. Mutual attraction among neighboring B cell receptors can arise due to antigen cross-linking, increased raft association upon antigen ligation, and other factors. We have simulated mutual attraction using a simple energy function given in the Methods section. The interaction energy is varied by changing the constant parameter K in the energy function. Receptor microclustering is observed for a wide range of parameter values and receptor concentrations. All of the simulations were performed for 10^8 time MC steps.

When we vary the K value for various receptor concentrations, lower K values did not lead to considerable microclustering. For high K values ($K \geq 2$), we observed small numbers of microclusters formed due to the intrinsic attractions among the receptor molecules (Figures 2 and S1 (Supporting Information)). Although at $K = 1$ small microclusters of four to five molecules are formed, they are transient in nature (Figure S1, Supporting Information). Qualitatively similar results are also obtained with eight neighboring nodes (Figure S4, Supporting Information). Interestingly, for $K = 3$ considering four neighboring nodes (Figure S2c, Supporting Information) and for $K = 2$ considering eight neighboring nodes (Figure S4b, Supporting Information), a single macrocluster of receptor molecules is formed irrespective of the receptor concentration in most repeats (trials) of our MC simulations. Thus, considering four neighboring nodes, $K = 3$ might be an optimal attraction energy that can lead to the formation of a very few large macroclusters. Below that attractive interaction strength, receptor attraction is too weak for a few large macroclusters to form that are stable over a long time. Above that value of the attractive interaction parameter, strong attraction among receptors within microclusters will make the microclusters quite stable over a long time so that the system is stuck in a metastable state of microclustered receptors.

We report all of the simulations obtained at $K = 4$ to understand the effect of receptor concentration. The microclusters once formed are stable over time, as depicted in Figure 3. With the increase of 10^7 time steps for $N = 100$ and $L = 30$, the initially formed five microclusters merged into two microclusters at 5×10^7 time steps and they are stable until the end of simulation. With the increase in the number of receptor molecules, the microclusters grow in size by accommodating an increasingly larger number of receptor molecules (Figure 4). When the receptor density is low, it leads to the microclustering. However, when we gradually increase the concentration of receptor molecules, fewer numbers of microclusters formed with increasing size and beyond a threshold concentration, a single macrocluster is formed. We also tested the nature of clustering with the increasing size of lattice from 15 to 75 for a given receptor number ($N = 100$) at different K values varied from 1 to 4. Results in this study were similar to those observed when we increased the number of receptors keeping the lattice size fixed.

For very high receptor concentration, local attraction between receptors can lead to receptor aggregation in a large macrocluster. However, such high receptor concentration may not be physiological. The radius of a typical B cell is 6 μm, and its surface area is 452.57 μm.^{2} The approximate number of B cell receptors per cell is 10^5. Each micrometer^2 surface area can have 221 molecules. We considered a grid of length

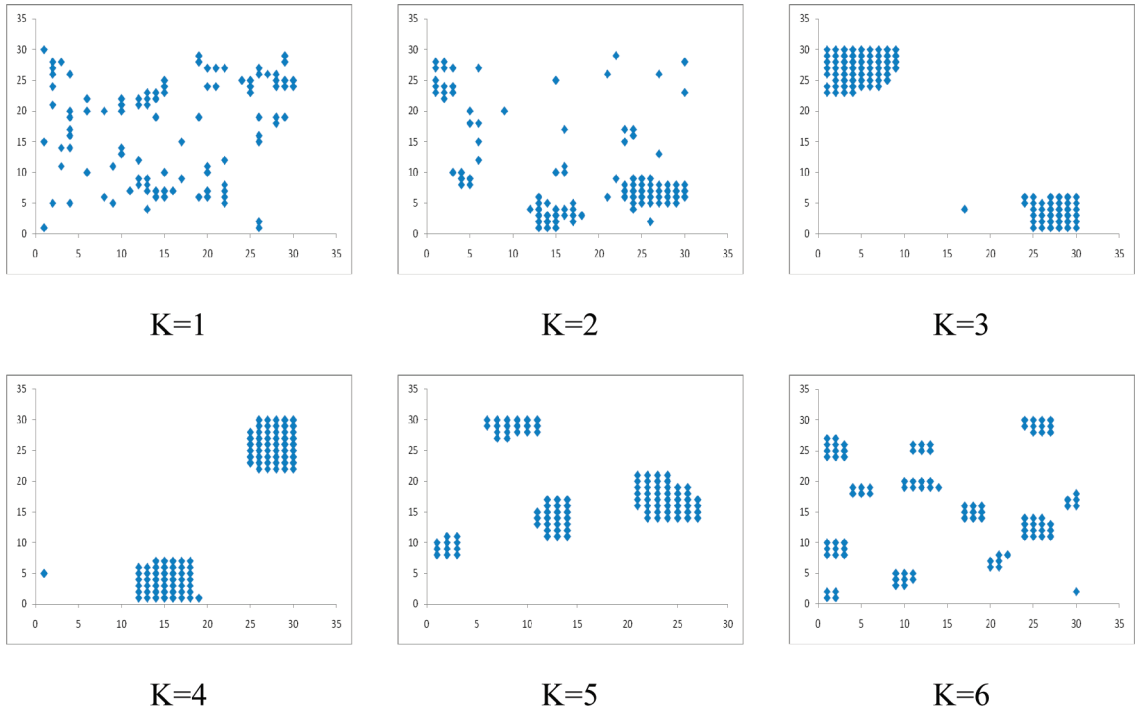

Figure 2. Microclustering of 100 cell receptor molecules with various K values after 10^8 Monte Carlo time steps ($N = 100$; $L = 30$; $T = 10^8$).

0.9 μm (area: 0.81 μm^2) with a grid spacing of 0.03 μm. Hence the approximate physiological concentration would be ~200 molecules on the full lattice.[12] Hence, a directed transport based mechanism is necessary for clustering on a larger scale.

Directed Bias toward the Largest Microcluster Leads to Receptor Macroclustering. Mutual attraction among neighboring receptors may not be enough to create macroclustering of B cell receptors such as what is seen in cap formations. We do not consider receptor attraction between receptor pairs that are spatially separated by large distances, as we do not find any direct biological mechanisms for such long-range attractions. Directed bias has been implicated in receptor clustering in the form of immune synapses in the case of T and B cells.[23,24] In those studies, for the case of membrane-bound antigens, receptor diffusion is thought to be biased toward the cell−cell contact region. In the case of soluble antigens, there is no cell−cell contact point and thus no such obvious preferred region toward which receptors would diffuse in a directed manner. This poses a challenge in selecting a direction for biased diffusion of B cell receptors. We assume that the largest microcluster that is formed at early times would trigger the strongest signaling inside a B cell and thus induce a directed transport toward that largest cluster. When we introduced such a biased diffusion toward the largest cluster, receptors aggregated in the form of a large microcluster (Figure S3, Supporting Information).

We also varied the probability (P_{bias}) with which the small microclusters move toward the largest microcluster. As depicted in Figure 5, for $N = 100$ and $L = 30$ when P_{bias} is less than 0.05, there was no macroclustering observed even if we run the simulation for a long time of 10^8 time steps. The minimum probability required for the formation of a macrocluster depends on the receptor concentration.

Network-Based Criteria to Characterize Receptor Micro- and Macroclustering. Spatial organization of B cell receptors on the cell surface can be considered as a dynamic network of receptors that changes during the course of receptor clustering and pattern formation. We show how a network-based metric can be used to quantitatively characterize various forms of receptor clustering: (i) random and uniform distribution of receptors, (ii) receptor microclustering, and (iii) receptor macroclustering.

Average Distance between Any Two Receptor Pairs. We propose that the average distance between any two pairs of receptors can be taken as a measure of receptor clustering. We derive two simple scaling relations for the two extreme cases (i) and (iii). The intermediate microclustering is found to be a linear combination of the two extreme cases. Clearly, receptor macroclustering (from an initial random distribution) would decrease the average distance between pairs of receptors, rendering this a quantitative measure of clustering. Interestingly, this average interpair distance also shows a simple scaling relation in terms of number of receptor molecules, but it is independent of other details such as the affinity of antigens.

(i) Random Distribution of Receptors. We can approximate the random receptor distribution as if the molecules are placed on a fully occupied two-dimensional square (Euclidean) lattice. The average separation distance between two neighboring receptors gives the node-to-node distance. In this approximation, the average distance between pairs of receptors is proportional to the lattice size L.[25]

$$\langle s \rangle \approx ln \qquad (l \text{ is the nodal spacing for an } n \times n \text{ lattice})$$
$$\approx L$$

Hence, the average separation distance does not decrease with an increase in the number of molecules. This is explained as a decrease in distance between neighboring receptors due to an increase in the number of molecules compensated by an increase in the number of molecules that are separated by large distances. However, any increase in system size L, i.e., the cell surface area, on which receptors are clustered will lead to an increase in the average separation distance between receptor pairs. This is verified in our

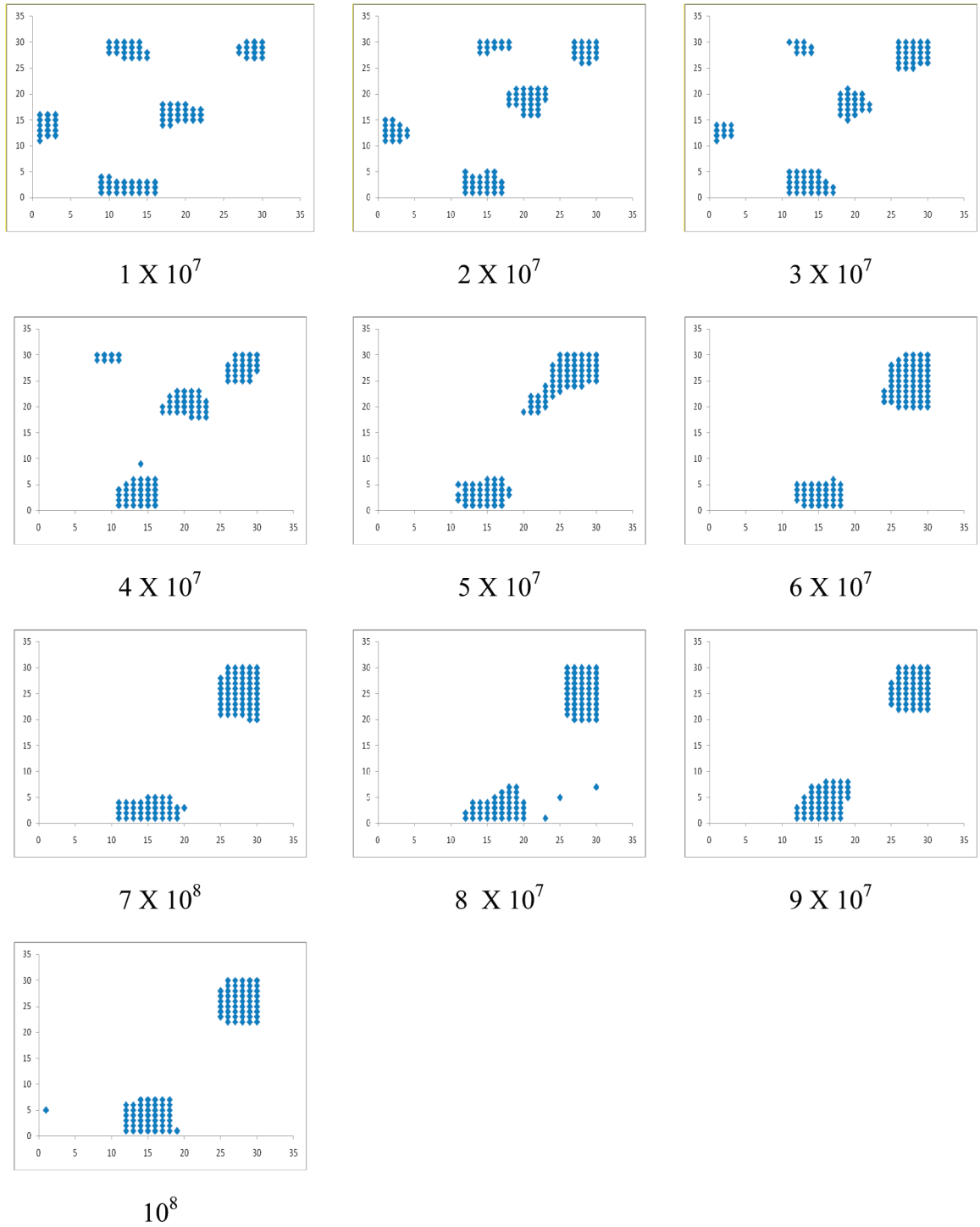

Figure 3. Snapshots of the receptor molecules at the regular time intervals (1×10^7 time steps) of the clustering simulations ($N = 100$; $L = 30$; $T = 10^8$; $K = 4$).

simulations, as shown in Figure 6. (a) When the lattice size is fixed at 30 and the number of molecules is increased from 100 to 500, the average interpair distance $\langle S \rangle$ does not depend on the number of molecules. (b) When the number of molecules is fixed at 100 and the lattice size is varied from 15−75, we observe a linear relationship between the average interpair distance and the lattice size with a slope value of 1.006 ± 0.0117.

(ii) Receptor Microclustering. This is an intermediate state of clustering where a set of receptor clusters are developed, each containing a few receptor molecules. An approximate estimation for cases with a small number of microclusters (2−3) shows the average interpair distance $\langle S \rangle$ to be a linear combination of two extreme cases of receptor clustering.

(iii) Receptor Macroclustering. In this case, we can again assume that the molecules are placed on a fully occupied two-dimensional square (Euclidean) lattice. However, the size of this occupied lattice increases with an increase in the number of molecules, as the clustering is limited by an intrinsic cutoff distance l_0 for neighboring receptor molecules. Physical exclusion of two B cell receptor molecules will set this cutoff distance l_0. In this regime of macroclustering, the average distance between any pairs of receptors is given by

$\langle s \rangle \approx l_0 n$ (l_0 is the nodal spacing for an $n \times n$ lattice)

$\langle s \rangle \approx l_0 N^{1/2}$ ($n^2 = N$, the total number of receptor molecules)

Thus, the proposed metric shows a power-law increase with the number of receptor molecules. To check the validity of our results, we varied the number of receptor molecules in our simulations.

Once the macroclusters are obtained from microclusters due to biased diffusion, the average interpair distance ($\langle S \rangle$) is plotted against the number of molecules (Figure 7a) and it is observed that $\langle S \rangle$ is directly proportional to the square root of the number of receptor molecules. The graph plotted on a log-scale confirms the power-law increase with an exponent of $\alpha = 0.510 \pm 0.0138$ (Figure 7a). Even though we develop this network-based metric of receptor clustering to specifically describe clustering of BCRs, the scaling relations obtained do not depend on the details of the system such as the antigen affinity. The average interpair distance $\langle S \rangle$ could not capture the microclustering as depicted in Figure 7b. Thus, we introduce a different measure which

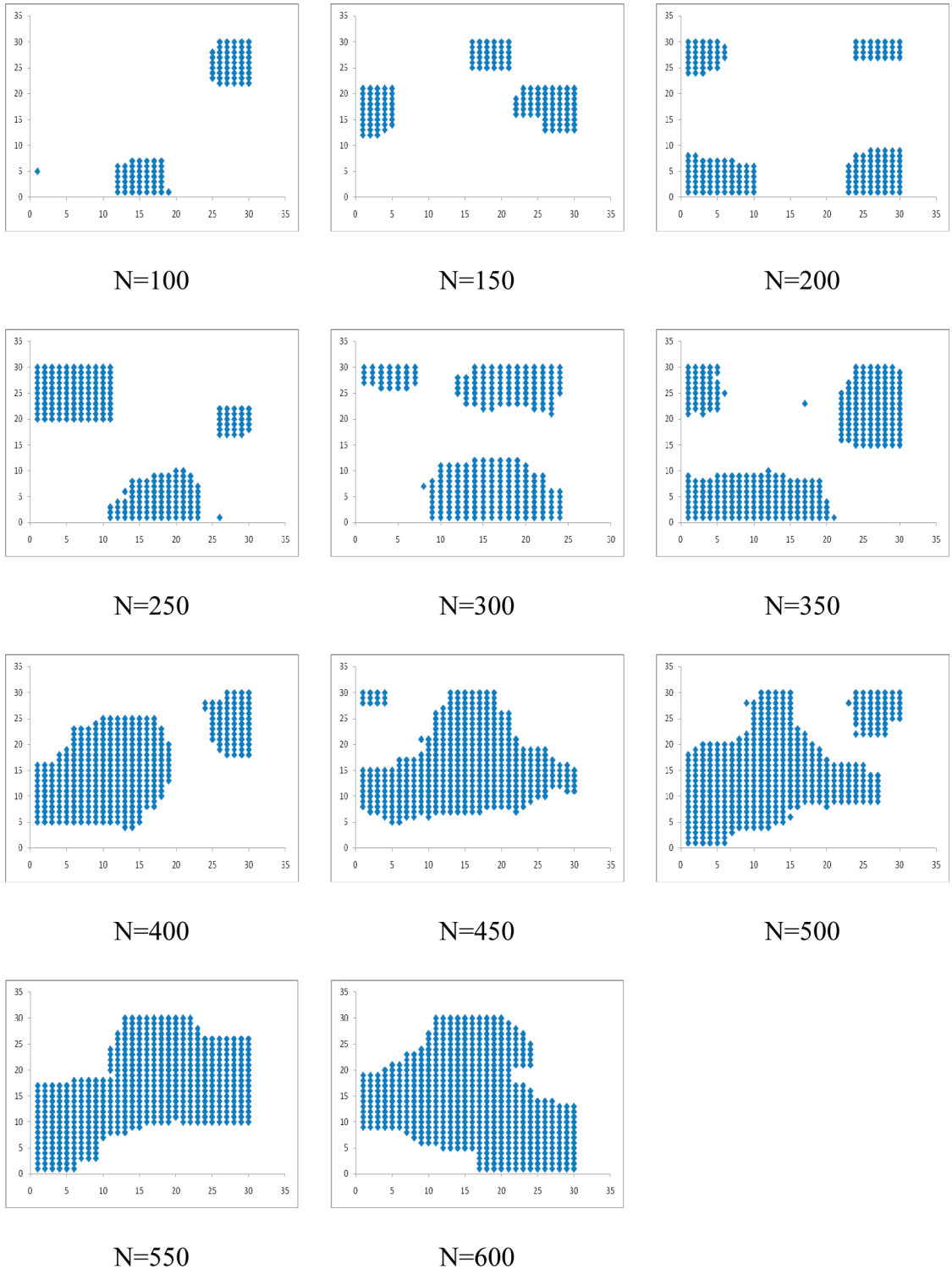

Figure 4. Snapshots of microclustering for various sets of receptor concentrations increasing the number of receptor molecules from 100 to 600 ($L = 30$; $T = 10^8$; $K = 4$).

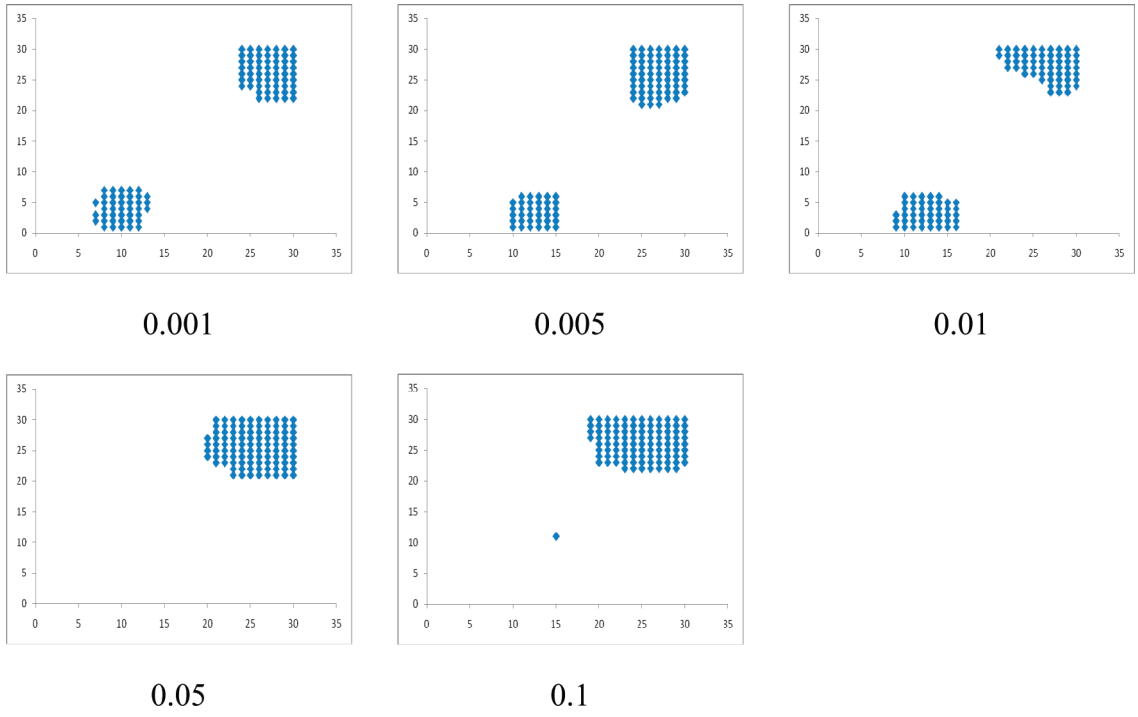

Figure 5. Snapshots of micro/macroclustering at different probabilities of diffusion (P_{bias}) for directed diffusion ($N = 100$; $L = 30$; $T = 10^8$; $K = 4$).

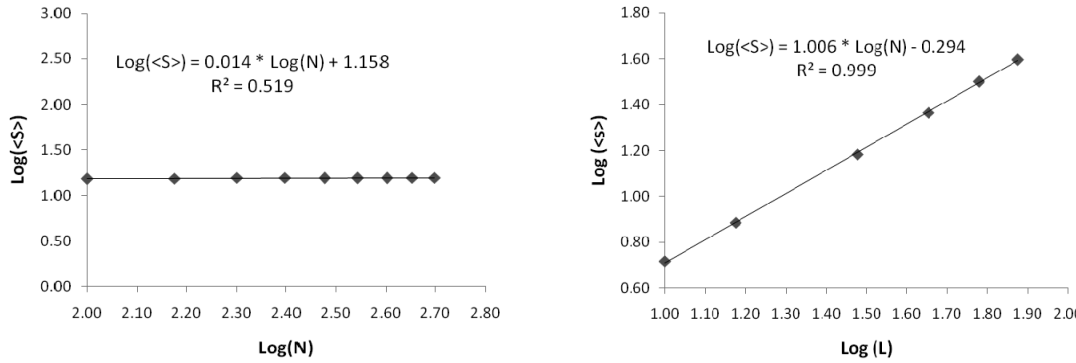

Figure 6. Plot depicting the change of average interpair distance $\langle S \rangle$ (a) with the change in the number of receptor molecules when the lattice size is 30 and (b) with the lattice size when the number of molecules is 100.

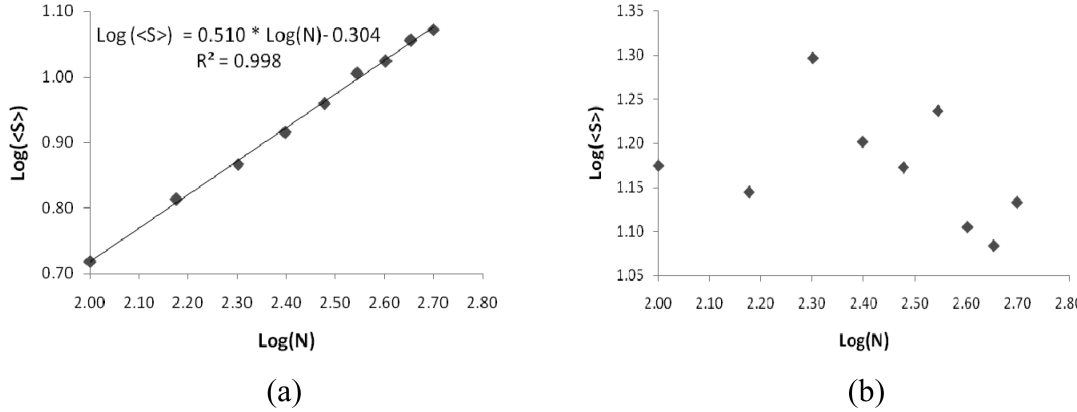

Figure 7. Plot depicting the change of average interpair distance $\langle S \rangle$ with the number of receptor molecules, when the receptor molecules are (a) macroclustered and (b) microclustered.

could capture the quantitative estimation of both macro- and microclustering.

Number of Adjacent Pairs $\langle P \rangle$**.** The number of adjacent molecular pairs also shows a simple scaling relation in terms of the number of molecules. As mentioned before, we can assume that the molecules are placed on a fully occupied two-dimensional square (Euclidean) lattice of size n. The number of molecular pairs, except for the pairs where both molecules

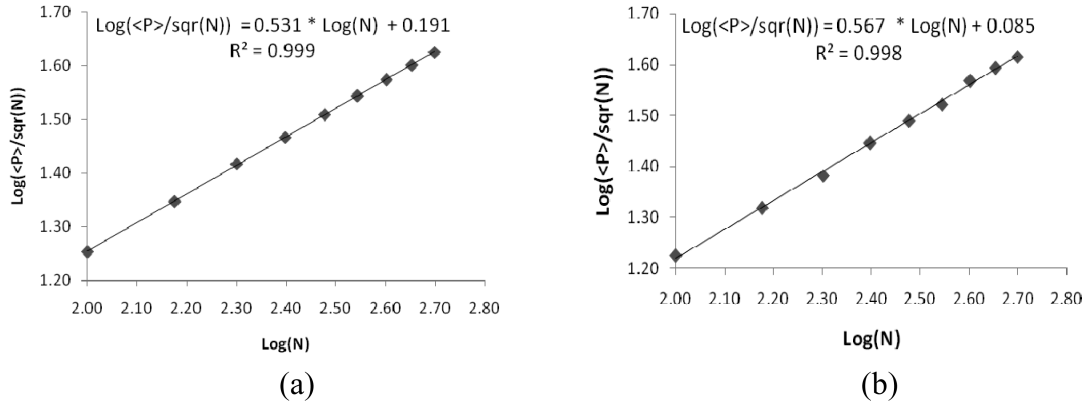

Figure 8. Plot depicting the change of adjacent number of pairs ($\langle P \rangle$) with the number of receptor molecules, when the receptor molecules are (a) macroclustered and (b) microclustered.

are residing on the boundary, is given by $2(n-2)(n-1)$. The number of molecular pairs at the boundary is $4(n-1)$. Hence, the total number of pairs is given by $2(n-2)(n-1) + 4(n-1) = 2(n^2 - n) = 2(N - N^{1/2})$. N is the total number of molecules; thus, $N = n^2$.

$$\text{number of pairs } \langle P \rangle = 2L(L-1) \quad (\text{when } L \geq 2)$$
$$= 2(N - \text{Sqrt}(N)) \quad (\text{when } N \geq 4)$$
$$\langle P \rangle/\text{Sqrt}(N) = 2(\text{Sqrt}(N) - 1) \sim 2(\text{Sqrt}(N)) \quad (\text{typically } N \gg 1)$$

$\langle P \rangle/\text{Sqrt}(N)$ is linearly proportional to $\text{Sqrt}(N)$.

The same is observed from our simulations when we plotted $\langle P \rangle$ /Sqrt(N) against the number of receptor molecules on a logarithmic scale (Figure 8); in the case of macroclustering, a linear relationship with a slope of 0.531 ± 0.005 is obtained. Similarly, for microclustering also, a linear curve is obtained with a slope value of 0.567 ± 0.011.

Discussion

In the present study, we have developed a simple model of B cell receptor clustering that occurs due to intrinsic attractions between spatially close receptor pairs and an additional late-time biased diffusion. A more detailed model with explicit cross-linking of B cell receptors by multivalent antigens is currently under investigation. In order to study receptor clustering in our effective mutual receptor attraction model, we developed a novel energy-function-based Monte Carlo technique. This proposed algorithm is biased toward large energy change moves so that the receptors cluster in a reasonable simulation time scale. The Monte Carlo study demonstrates the formation mechanism of the microclusters as we vary the strength of receptor−receptor attraction as well as the receptors/antigen density.

However, microclusters formed due to such receptor−receptor attractions do not coarsen into a large macrocluster except for very specific parameter values such as very high antigen concentrations. When the formed microclusters are directed toward the largest microcluster, it leads to a cap formation (macrocluster). Even though formation of a receptor macrocluster under biased diffusion directed toward a specific region on the cell surface is somewhat obvious, the initial choice of that preferred location on a spherically symmetric cell surface is far from being obvious. For the case of receptor clustering at the intracellular junction, between two cells in contact, the obvious choice for directed transport is the cell−cell contact region. In contrast, for receptor clustering in B cells, upon ligation with soluble antigens, the preferred location of receptor transport is difficult to determine, especially due to lack of suitable experimental studies.[11] We are currently exploring different possible mechanisms of directed diffusion using the above-mentioned detailed model of BCR clustering that simulates BCR cross-linking by multivalent antigens.

The designed receptor network measures (a) the average distance between receptor pairs $\langle S \rangle$ and (b) the number of adjacent pairs $\langle P \rangle$ could effectively yield quantitative estimates for different types of receptor clustering. The same network-based measures can be used to analyze experimental data on B cell receptor clustering that could thus connect experimental results with our computational studies. Imaging studies could yield position information B cell receptors on the cell surface in a dynamic manner as they organize into clusters. Such position information can be used to estimate both the average distance and the number of adjacent pairs. In addition, recent FRET experiments that used either (i) Ig-α GFP and Ig-β YFP or (ii) Ig-α GFP and Ig-α YFP can both indicate receptor clustering and can be well correlated with the number of adjacent pairs of receptors calculated in our theoretical modeling study.

Acknowledgment. A.S.R. acknowledges support from National Institutes of Health grant AI074022.

Supporting Information Available: The results obtained with different binding strength values (K) and considering the eight neighboring nodes. This material is available free of charge via the Internet at http://pubs.acs.org.

References and Notes

(1) Ashkenazi, A.; Dixit, V. M. *Science* **1998**, *281*, 1305.
(2) Humphries, M. J. *Curr. Opin. Cell Biol.* **1996**, *8*, 632.
(3) Guo, C.; Levine, H. *Biophys. J.* **1999**, *77*, 2358.
(4) Unanue, E. R.; Karnovsky, M. J. *J. Exp. Med.* **1974**, *140*, 1207.
(5) Schamel, W. W.; Reth, M. *Adv. Exp. Med. Biol.* **2008**, *640*, 64.
(6) Yokosuka, T.; Saito, T. *Immunol. Rev.* **2009**, *229*, 27.
(7) Monks, C. R.; Freiberg, B. A.; Kupfer, H.; Sciaky, N.; Kupfer, A. *Nature* **1998**, *395*, 82.
(8) Grakoui, Bromley, S. K.; Sumen, C.; Davis, M. M.; Shaw, A. S.; Allen, P. M.; Dustin, M. L. *Science* **1999**, *285*, 221.
(9) Batista, F. D.; Iber, D.; Neuberger, M. S. *Nature* **2001**, *411*, 489.
(10) Batista, F. D.; Harwood, N. E. *Nat. Rev. Immunol.* **2009**, *9*, 15.
(11) Tolar, P.; Sohn, H. W.; Pierce, S. K. *Immunol. Rev* **2008**, *221*, 64.
(12) (a) Tsourkas, P. K.; Longo, M. L.; Raychaudhuri, S. *Biophys. J.* **2008**, *95*, 1118. (b) Tsourkas, P. K.; Baumgarth, N.; Simon, S. I.; Raychaudhuri, S. *Biophys. J.* **2007**, *92*, 4196.
(13) Treanor, B.; Batista, F. D. *Curr. Opin. Immunol.* **2007**, *19*, 476.
(14) Dustin, M. L. *Immunity* **2009**, *30*, 482.

(15) Goldstein, B.; Faeder, J. R.; Hlavacek, W. S. *Nat. Rev. Immunol.* **2004**, *4*, 445.

(16) Schreiner, G. F.; Fujiwara, K.; Pollard, T. D.; Unanue, E. R. *J. Exp. Med.* **1977**, *145*, 1393.

(17) Dykstra, M.; Cherukuri, A.; Sohn, H. W.; Tzeng, S.-J.; Pierce, S. K. *Annu. Rev. Immunol.* **2003**, *21*, 457.

(18) Schmidt, C.; Kim, D.; Ippolito, G. C.; Naqvi, H. R.; Probst, L.; Mathur, S.; Rosas-Acosta, G.; Wilson, V. G.; Oldham, A. L.; Poenie, M.; Webb, C. F.; Tucker, P. W. *EMBO J.* **2009**, *28*, 711.

(19) Depoil, D.; Fleire, S.; Treanor, B. L.; Weber, M.; Harwood, N. E.; Marchbank, K. L.; Tybulewicz, V. L. J.; Batista, F. D. *Nat. Immnol.* **2008**, *9*, 63.

(20) Tolar, P.; Hanna, J.; Krueger, P. D.; Pierce, S. K. *Immunity* **2009**, *30*, 44.

(21) Sohn, H. W.; Tolar, P.; Jin, T.; Pierce, S. K. *Proc. Natl. Acad. Sci. U.S.A.* **2006**, *103*, 8143.

(22) Newman, M. E. J.; Barkema, G. T. *Monte Carlo Methods in Statistical Physics*; Oxford University Press: New York, 1999.

(23) Wulfing, C.; Davis, M. M. *Science* **1998**, *282*, 2266.

(24) Fleire, S. J.; Goldman, J. P.; Carrasco, Y. R.; Weber, M.; Bray, D.; Batista, F. D. *Science* **2006**, *312*, 738.

(25) Newman, M. E. J. *J. Stat. Phys.* **2000**, *101*, 819.

JP9079074